

 Open access • Journal Article • DOI:10.1103/PHYSREVE.80.061914

Spontaneous Brain Activity as a Source of Ideal 1/f Noise — [Source link](#)

Paolo Allegrini, Danilo Menicucci, Remo Bedini, Leone Fronzoni ...+5 more authors

Institutions: [University of Pisa](#), [Sant'Anna School of Advanced Studies](#), [University of North Texas](#), [Duke University](#)

Published on: 18 Dec 2009 - [Physical Review E](#) (American Physical Society)

Related papers:

- [Self-organized criticality: An explanation of the 1/ f noise](#)
- [Neuronal Avalanches in Neocortical Circuits](#)
- [Maximizing information exchange between complex networks](#)
- [Mosaic organization of DNA nucleotides](#)
- [Fractal complexity in spontaneous EEG metastable-state transitions: new vistas on integrated neural dynamics](#)

Share this paper:    

View more about this paper here: <https://typeset.io/papers/spontaneous-brain-activity-as-a-source-of-ideal-1-f-noise-1svp3mwjn5>

Spontaneous brain activity as a source of ideal $1/f$ noise

Paolo Allegrini,^{1,2} Danilo Menicucci,^{1,3} Remo Bedini,^{1,3} Leone Fronzoni,² Angelo Gemignani,^{1,3,4} Paolo Grigolini,⁵
Bruce J. West,⁶ and Paolo Paradisi⁷

¹*Istituto di Fisiologia Clinica (IFC-CNR), Via Moruzzi 1, 56124 Pisa, Italy*

²*Dipartimento di Fisica "E. Fermi," Università di Pisa and INFN CRS-SOFT, Largo Pontecorvo 3, 56127 Pisa, Italy*

³*Centro EXTREME, Scuola Superiore Sant'Anna, P.zza Martiri della Libertà 7, 56127 Pisa, Italy*

⁴*Department of Physiological Sciences, University of Pisa, Via San Zeno 31, 56127 Pisa, Italy*

⁵*Center for Nonlinear Science, University of North Texas, P.O. Box 311427, Denton, Texas 76203, USA*

⁶*Physics Department, Duke University, Durham, North Carolina 27708, USA*

⁷*Istituto di Scienze dell'Atmosfera e del Clima (ISAC-CNR), Lecce Unit, Strada Provinciale Lecce-Monteroni km 1.2, I-73100 Lecce, Italy*

(Received 6 August 2009; revised manuscript received 19 October 2009; published 18 December 2009)

We study the electroencephalogram (EEG) of 30 closed-eye awake subjects with a technique of analysis recently proposed to detect punctual events signaling rapid transitions between different metastable states. After single-EEG-channel event detection, we study global properties of events simultaneously occurring among two or more electrodes termed coincidences. We convert the coincidences into a diffusion process with three distinct rules that can yield the same μ only in the case where the coincidences are driven by a renewal process. We establish that the time interval between two consecutive renewal events driving the coincidences has a waiting-time distribution with inverse power-law index $\mu \approx 2$ corresponding to ideal $1/f$ noise. We argue that this discovery, shared by *all subjects* of our study, supports the conviction that $1/f$ noise is an optimal communication channel for complex networks as in art or language and may therefore be the channel through which the brain influences complex processes and is influenced by them.

DOI: [10.1103/PhysRevE.80.061914](https://doi.org/10.1103/PhysRevE.80.061914)

PACS number(s): 87.85.dm, 89.75.Da, 87.19.le

I. INTRODUCTION

The phenomenon of inverse-power-law power spectra, termed $1/f$ noise, is believed by many to be the signature of complexity. Herein we retain the commonly used term *noise*, even though, one might argue, we should more appropriately use the term *signal*, since the phenomenon naturally emerges from data produced by complex systems. Leaving this argument aside, we elect to describe the spectrum of variability of the most complex network of all, the human brain, as $1/f$ noise. We further note that in literature, and also in the case of the physiological processes driven by the brain, some researchers use the term $1/f^\eta$ rather than $1/f$ noise [1], implying that $1/f$ is a particular condition corresponding to $\eta=1$, while many other authors use the term $1/f$ noise to refer to inverse-power-law power spectra regardless of the index. To minimize the confusion caused by this extended definition of $1/f$ noise, we shall throughout adopt the latter definition and refer to the case $\eta=1$ as *ideal* $1/f$ noise, since real complex networks generate noise in a range $0.5 < \eta < 1.5$.

A. $1/f$ noise in the brain

The origins of $1/f$ noise have challenged theoretical physicists for the past century. As far as neural dynamics is concerned, for example, the fluctuating reaction times generated by the cognitive processes stimulated by psychological tests have a $1/f$ noise character [2,3]. It is not yet determined if these highly correlated fluctuations are generated either by the oscillatory neural synchronization advocated by Medina [4] or by the spontaneous phase-transition process of many interacting neurons proposed by Bianco *et al.* [5], or by yet to be uncovered complex dynamic processes. The phase-

transition conjecture fits the criticality condition stressed in the recent neurophysiological literature (see, e.g., Ref. [6]). This condition will be discussed in some detail in Sec. V.

Many authors have investigated the brain dynamics via the analysis of electroencephalogram (EEG) records either studying the time decay of the autocorrelation function, or, alternatively, by directly studying its Fourier transform, i.e., the power spectrum. The latter measure records inverse-power-law spectral indexes η ranging from 0.36 to values slightly larger than 1.0 [2,7,8]. In particular, the authors of Ref. [8] studied the correlation function using a data-driven diffusion technique similar to the one that we propose herein and evaluated the EEG spectrum in the open-eyes condition. They found values of η slightly larger than 1, suggesting, as will become clear subsequently, that the brain lives in a non-stationary nonergodic condition.

The differences in the values of the inverse power-law indices obtained for the brain can be explained in part by the fact that a variety of physiological conditions and techniques have been used. However, from the experimental finding of the condition $\eta > 1$ in Ref. [8] one may draw some conclusions about the origin of $1/f$ noise, which, in turn, clarifies why the evaluation of the index η is so elusive.

We remark that the condition $\eta > 1$ is not compatible with stationary autocorrelation functions and that a direct application of the Wiener-Kinchine theorem to brain wave data leads to the paradoxical consequence of correlations indefinitely growing in time. The only available theoretical approach compatible with the experimental observation of $\eta > 1$ makes recourse to renewal events. We stress that this approach is able to explain the extended memory implied by $1/f$ noise, even in the extreme condition of $\eta > 1$, as will be discussed in Secs. II and V.

B. $1/f$ noise from renewal events

It is thought that the $1/f$ noise observed throughout human physiology and behavior reflects the coordinative, metastable basis of cognition [9,10]. In Sec. III we further discuss the metastability of the EEG signal for the purpose of illustrating the transitions from one to another metastable state realized though abrupt changes that are the candidates of renewal events to detect.

Let us consider a sequence of events characterized by their occurrence times $\{t_n\}$, or, alternatively, by the sequence $\{\tau_n\}$ of time intervals between successive events. These events are said to be *renewal* if all $\tau_i \in \{\tau_n\}$ are mutually statistically independent random variables, a property that, as shown in Sec. V, does not conflict with the existence of a very extended memory [11]. Following Lowen and Teich [12], let us assume that the interval between two consecutive events is described by a waiting-time distribution density $\psi(\tau)$, which becomes proportional to $1/\tau^\mu$ for $\tau \rightarrow \infty$. We denote the moments of the waiting time by

$$\langle \tau^n \rangle = \int \tau^n \psi(\tau) d\tau. \tag{1}$$

Let us focus our attention on

$$1 < \mu < 3, \tag{2}$$

which makes the second moment $\langle \tau^2 \rangle$ diverge. We refer throughout to these events as *crucial*, since, as discussed in Secs. II and V, signals driven by such events show long-time correlations called *intermittency* in the physics literature. Notice that the condition $\mu < 2$ implies the first moment $\langle \tau \rangle$ diverges as well, with an even more striking departure from the conditions of ordinary statistical physics. This condition yields such an extended memory that the system is in fact incompatible with the existence of equilibrium, whereas for the condition $2 < \mu < 3$ equilibrium exists, but it takes an infinitely long time to reach it from an initial out-of-equilibrium condition [13].

Renewal events may be used to generate an *artificial signal* $\xi(t)$, with a power spectrum $1/f^\eta$, where η depends on the rules adopted to generate the signal. We report on the theoretical predictions for η , i.e., the spectral index of the artificial signal, as a function of μ , i.e., the index for the renewal statistics. In Sec. II we provide methods of analysis to compute μ using the same artificial-signal methodology.

Let us call *laminar regions* the time intervals between two consecutive crucial events. Consider now the case when the signal $\xi(t)$ vanishes in the whole laminar region, and it achieves a nonvanishing constant value only at the times when a crucial event occurs, namely, the case where the signal is a sequence of pulses of constant intensity. For this artificial signal the power-law index is given for various values of the renewal index

$$\eta = \begin{cases} \mu - 1 & \text{if } 1 < \mu < 2 \\ 3 - \mu & \text{if } 2 \leq \mu \leq 3 \\ 0 & \text{if } \mu > 3. \end{cases} \tag{3}$$

If we adopt a different prescription to generate the signal $\xi(t)$, by assigning to each laminar region either the value 1 or

-1, according to a coin-tossing procedure [14], we have the spectral index

$$\eta = 3 - \mu. \tag{4}$$

It is interesting to notice that when

$$\mu = 2 \tag{5}$$

we obtain ideal $1/f$ noise in both cases. It is also interesting to notice that Eq. (4) is compatible with a range of values $0 < \eta < 2$ and in particular is able to yield $\eta > 1$ if $\mu < 2$. We stress, and we shall come back to this point in Sec. II, that the artificial signal ought not to be confused with a model for the signal under study, from which events have been detected. The artificial signal is intended to demonstrate how $1/f$ noise and renewal processes can be related in general.

The direct evaluation of the $1/f$ -index η from signals generated by renewal events is a delicate task. Margolin and Barkai [15] adopted the prescription leading to the relation between indices [Eq. (4)] and pointed out the irretrievably nonstationary character of the underlying process for the condition $\mu < 2$. In spite of this nonstationarity they succeeded in generalizing the Wiener-Kinchine theorem, whose ordinary form holds true only in the stationary case. They also derived for the spectrum $P(f)$, when $\mu < 2$,

$$P(f) \propto \frac{1}{f^{3-\mu} L^{2-\mu}}, \tag{6}$$

where L is the length of the time series under study. In this case the longer the sequence, the weaker the noise intensity. Lukovic and Grigolini [16] supported this conclusion and emphasized the nonstationary character of the whole region (2) of parameter values. Nonstationary effects are not easily revealed for μ significantly larger than 2, where the spectrum $P(f)$ is virtually independent of the sequence length L . However, the nonstationary nature of the process becomes strong as we approach the unique value $\mu=2$ either from above or from below thereby requiring the average over many realizations of the underlying physical process. This suggests why the spectrum of a single EEG is never smooth.

As an indirect indication of the presence and fundamental role of crucial events, we note that neuron systems have been determined to be more sensitive to $1/f$ signals than to white noise [17]. This observation is consistent with the complexity matching (CM) principle, according to which the transmission of information preferentially occurs between complex networks with the same complexity (i.e., the same μ index) [13], due to the actions of renewal events.

C. Complexity matching

There is general agreement that the brain is a source of $1/f$ noise [13]. This perspective also suggests why $1/f$ spectra are present in language and in the artwork of the masters [18], which are a product of the creativity and variability of the brain. Using the CM principle [13], understanding why music exerts its spell on the brain [19] becomes evident as well. In fact, it is well known that music generates $1/f$ spectra [20] and some authors believe in the so-called ‘‘Mozart effect,’’ namely, that certain types of music may correlate

with higher levels of creative and analytic reasoning and more generally with intelligence [21]. The neural foundation of the decision making processes [22] is, at the same time, of fundamental importance for the emerging science of neuroeconomics [23], which revives some of the pioneering ideas of Samuelson [24].

The authors of Ref. [25] established a connection between Zipf's law in natural human language and the scale-free semantic networks [26] leading to the conclusion that the ideal Zipf's law corresponds to the boundary value $\mu=2$. The small excursions above the boundary ensure the stability necessary for *learnability* and those below the boundary make it possible to explore a virtually infinite cognitive space thereby allowing language to evolve. It is worth mentioning that there exists a close connection between Zipf's law and phase-transition processes. Cancho and Solé [27] have proposed a dynamic approach to Zipf's law based on a control parameter λ denoting the speaker (λ) and hearer ($1-\lambda$) in the communication effort. At a critical value λ^* a phase transition occurs corresponding to the emergence of Zipf's law.

D. Purpose and outline of the paper

All this background is attractive and exciting, but the fact remains that it is not yet proved in a way that has been universally accepted that the brain generates $1/f$ noise. Proving that the brain's $1/f$ noise emerges from the renewal condition would provide a solid foundation for the science of socioneurophysiological processes. However, proving that the brain's $1/f$ noise is renewal and based on nonstationary fluctuations is a source of confusion, affected by statistical errors, making a direct proof extremely difficult. The main purpose of this paper is to afford this proof, and to do that, for the reasons earlier discussed, we have to find an alternative procedure to the direct evaluation of the spectrum.

The outline of the paper is as follows. In Sec. II we review the rules for a random walk process used to generate a diffusion process from a sequence of events and we give theoretical predictions for the scaling coefficients of the processes in terms of the renewal index μ . In Sec. III we give details on how to identify the events with rapid transitions between global EEG metastable states. In Sec. IV we show how scaling parameters are detected from such events. In Sec. V we recall some recent findings suggesting that the brain is a system at a critical transition point, and we discuss how renewal properties naturally emerge in critical systems. These renewal processes are in turn responsible for very extended memory as we explain. Finally, in Sec. VI we illustrate the trade-off among different prescriptions yielding the main result of this paper, that the dynamics of the brain is driven by renewal events with $\mu=2$.

II. EVENT-DRIVEN RANDOM WALKS

In Sec. I we mentioned two prescriptions to generate an event-driven signal $\xi(t)$. We again alert the reader to the fact that none of these rules is expected to exactly correspond to a brain generated signal. These rules show to what an extent

ideal artificial signals driven only by crucial events generate a diffusion process whose scaling properties depend on the statistics of crucial events. Note, for instance, that with the rule yielding Eq. (4) we generate a signal that does not seem to bear a direct connection with crucial events insofar as the occurrence of an event does not necessarily generate a jump. In fact, at the moment when an event occurs, the fluctuation $\xi(t)$ with probability of 1/2 may keep the same sign as in the earlier laminar region. Although the signal $\xi(t)$ obtained by filling the laminar regions with alternate signs may seem to establish a more direct connection with crucial events, we do not propose either of them to model brain's dynamics.

In fact, we use the walking rules as a procedure to measure the complexity of *coincidences*, and these coincidences are real brain events detected by means of the procedure described in Sec. III. This analysis, as we discuss herein, is robust against the fact that some events may not be detected and that we may also have artifactual *false positives*. As far as a model is concerned, crucial events may trigger some complicated dynamics which may, at the level of the signal, create a distortion of the detected value of η . This will be the subject of further studies. However, we argue that the long-time properties of the signal are probably completely dominated by the action of crucial events.

In this section we review the exact theoretical predictions stemming from renewal theory, which are the basis of the methods of analysis used in Sec. IV. Following the suggestions of the authors of Refs. [28,29], in addition to the rules of Eqs. (3) and (4), we find it useful to adopt a third rule proposed by the authors of Ref. [30]. The random walker at the moment of an event occurrence can either make a jump forward or backward according to a coin-tossing prescription. These three rules make the diffusing variable $x(t) = \int_0^t \xi(t') dt'$ yield different scaling coefficients [28].

The statistical properties of the variable $x(t)$ are related to the autocorrelation function of the signal itself via

$$C(t) \equiv \frac{\langle y(0)y(t) \rangle}{\langle y^2 \rangle} = \frac{1}{2} \frac{d^2[\langle \Delta x^2(t) \rangle - \langle \Delta x(t) \rangle^2]}{dt^2}, \quad (7)$$

where $y = \xi - \langle \xi \rangle$, and $\Delta x \equiv x(t_w + t) - x(t_w)$, t_w denoting the beginning of the moving windows, over which the statistics are built and averages $\langle \cdot \rangle$ are performed (time averages). The Fourier transform of $C(t)$ is the power spectrum. The function $p(\Delta x, \Delta t)$ is the probability density of finding a displacement around Δx in a time window of length Δt . We have a scaling relation if

$$p(\Delta x, \Delta t) = F\left(\frac{\Delta x}{\Delta t^\delta}\right) \frac{1}{\Delta t^\delta}, \quad (8)$$

where $F(x)$ is a normalized distribution density. The first factor on the right-hand side of Eq. (8) tells us that $\Delta x \sim \Delta t^\delta$, while the second factor is only normalization. It is useful to study the second moment of the displacement, namely, the function which is differentiated twice in Eq. (7) defining an index H via

$$\langle \Delta x^2(\Delta t) \rangle - \langle \Delta x(\Delta t) \rangle^2 = K \Delta t^{2H}, \quad (9)$$

where K is a constant. If the scaling was perfect, as in fractional Brownian motions, $H = \delta$. When the diffusion process is driven by renewal events, H and δ are slightly different in the $1/f$ regime studied herein. It is, however, always true that Eq. (9), making use of Eq. (7) and of a Tauberian theorem, yields $\eta = 2H - 1$ and that $H \approx \delta$ when $\eta \approx 1$, namely, in the case of ideal $1/f$ noise. Notice further that the generated artificial signal has long-range correlations when $H \neq 0.5$.

With rule no. 1, termed the asymmetric jump (AJ) in Ref. [28], the signal is kept constant with $\xi(t) = 0$ within the laminar region and $\xi(t) = 1$ at the time of an event occurrence. This rule generates

$$\delta = \mu - 1, \quad H = \frac{\mu}{2} \quad (10)$$

for $1 < \mu < 2$ and

$$\delta = \frac{1}{\mu - 1}, \quad H = 2 - \frac{\mu}{2} \quad (11)$$

for $2 < \mu < 3$.

With rule no. 2, termed the symmetric velocity (SV) in [28], the signal is kept constant with $\xi(t) = \pm 1$ within the laminar region, and a change in sign may or may not occur, at the time of an event occurrence, according to a coin-tossing procedure. This rule yields

$$\delta = 1, \quad H = 2 - \frac{\mu}{2} \quad (12)$$

for $1 < \mu \leq 2$ and

$$\delta = \frac{1}{\mu - 1}, \quad H = 2 - \frac{\mu}{2} \quad (13)$$

for $2 < \mu < 3$. It is important to stress that for $\mu < 2$ the second-moment prediction is apparently unphysical given the fact that in the traditional stationary case the scaling $H = 1$, the well known ballistic condition, is the impassable maximum scaling value: no diffusion can spread faster than walkers running with constant velocity with no direction change. However, if we abandon the traditional stationary perspective and we take into account the ergodicity breakdown generated by $\mu \leq 2$ we find that this apparently impassable limit can be overcome [31].

Finally, with rule no. 3, termed the symmetric jump (SJ) in [28], the signal is kept constant with $\xi(t) = 0$ within the laminar region and $\xi(t) = \pm 1$ at the time of an event occurrence selected by coin tossing. This rule generates

$$\delta = H = \frac{\mu - 1}{2} \quad (14)$$

for $1 < \mu \leq 2$ and

$$\delta = H = \frac{1}{2} \quad (15)$$

for $\mu > 2$.

To establish our claim that the brain is the source of ideal $1/f$ noise we have to find a sequence of brain events that are global [32] and not specifically related to a single function. Then we have to prove that the diffusion processes generated by rules no. 1, no. 2, and no. 3 yield $\delta = H = 1$, $\delta = H = 1$, and $\delta = H = 0.5$, respectively.

The joint use of these different rules allows us to settle some ambiguities. According to the authors of Ref. [28] the method of diffusion entropy (DE) that we shall revise in Sec. IV A becomes an accurate scaling detector when rule no. 1 (AJ) is used. However, we see that according to Eqs. (10) and (11) of rule no. 1, the same value of δ fitting the condition $0.5 < \delta < 1$ is compatible with both $\mu = 1 + \delta < 2$ and $\mu = 1 + 1/\delta > 2$, respectively, thereby assigning to rule no. 3 (SV) or no. 2 (SJ) the crucial role of establishing if $\mu > 2$ or $\mu < 2$ given the fact that in the former case rule no. 3 would yield $\delta = (\mu - 1)/2 < 0.5$ and in the latter $\delta = 1$. The detection of H for the signal generated using rule no. 1 (AJ) is affected by a similar ambiguity for the evaluation of μ . The comparison of the three rules, as will become clear in Sec. IV, makes the analysis able to deal with spurious events, which can be treated as superimposed noise.

We shall see that in addition to the nonergodic nature of the condition $\mu \leq 2$, we have to take into account also an additional form of nonstationary behavior represented by nonstationary drifts in the signal. For this reason we shall follow the advice of the authors of [33] and evaluate both the scaling index δ using the DE method [28] and the second-moment index H by means of the well known detrended fluctuation analysis (DFA) [34]. As we shall see, this has the effect of reducing the influence of the nonstationary drifts.

III. SEARCH FOR THE RAPID TRANSITION PROCESSES: DETAILS ON THE METHOD

A. General remarks

How can we detect a sequence of cerebral events that may be good candidates for satisfying all the above properties? We examine the EEG of 30 closed-eye subjects, namely, sequences characterized by the presence of “trains” of α waves. All subjects signed an informed consent according to the University of Pisa Ethical Committee guidelines. In the neurophysiological literature there is increasing conviction that brain dynamics is characterized by quakes [35] and avalanches [36–38]. The authors of Ref. [39] have recently proposed a method of analysis of electroencephalograms (EEG) and magnetoencephalograms (MEG) whose task is to identify the time points at which the EEG/MEG amplitude abruptly changes. These authors call these events *rapid transition processes* (RTPs). The RTPs have a short time duration and have been treated by them as point or near-point events. However, a thorough study on single channels shows significant variability among channels and among subjects [40]. Moreover, single-channel RTPs are not assumed to provide information on global brain processes thought to be associated with cognition. For this reason we make the key conjecture that the multichannel RTPs (MC-RTPs), defined as the temporal RTP coincidences among different channels, are the real source of $1/f$ spectra.

The EEG signal has, in general, time varying statistical properties; i.e., it is nonstationary. Some research work [39] suggests that the basic source of the observed nonstationarity in EEG signals is not due to the influences of external stimuli on the brain but it rather reflects the switching among metastable states of neural assemblies during brain functioning. According to this scenario a neuronal assembly is a group of neurons for which coordinated activity persists over substantial time intervals and underlies basic operations of information processing. At the level of EEG recordings these intervals should be reflected in periods of quasistationary signals. The occurrence of a crucial event represents the abrupt transition from one stationary condition to another. The majority of crucial events is associated with transition intensity of moderate size and remains unnoticed.

B. Segmentation of the EEG signals

Herein, with the term “segmentation” we mean the procedure by which each EEG signal has been processed to unveil its hidden piecewise stationary structure. In other words, segmentation means looking for the abrupt changes in EEG amplitude (RTPs) that glue together quasistationary EEG signal segments. The EEG segmentation method adopted herein is derived by the two-stage procedure proposed by Kaplan and co-workers in [39]. The segmentation algorithm is composed of two main stages: (1) a preliminary identification of the RTPs; (2) a selection of the actual RTPs on the basis of the steepness of the previously detected EEG amplitude changes. We remark that this method is nonparametric; i.e., it does not require parameter estimation of a given mathematical model for the detections of abrupt changes in EEG amplitude. Moreover, it is adaptive, since it uses local statistics of the signal around each detected point.

Stage (1) consists of two steps: (1a) the estimation of the envelope (i.e., the local amplitude) of each EEG signal and (1b) the detection of the abrupt changes in the EEG local amplitude time series. Step (1a) is performed applying the Hilbert transform [41] to the EEG signal and considering the modulus of the corresponding analytic signal. The obtained series constitutes the so-called *test sequence* (TS) [42], whose modifications are analyzed in step (1b). Step (1b), the basic procedure of segmentation, rests on comparing the ongoing instantaneous amplitude series with its average level over a surrounding window. To this aim, a smoothed test sequence termed *level sequence* (LS) has been derived from the previous one with an even-weighted moving-average filter (700 msec window length). In the case of rapid amplitude changes in the EEG, the LS will update its values with time delay with respect to the nonsmoothed TS. The time locations of each intersection between TS and LS can thus be considered as preliminary RTPs [39].

Stage (2) aims at overcoming a first step pitfall: some of the intersections between the two series do not correspond to a discontinuity between quasistationary EEG segments and thus false RTPs, related to brief anomalous peaks in the test sequence, may occur. According to Kaplan *et al.* [39], anomalous peaks (either related to very tight pairs of intersections or without a steady separation between the two se-

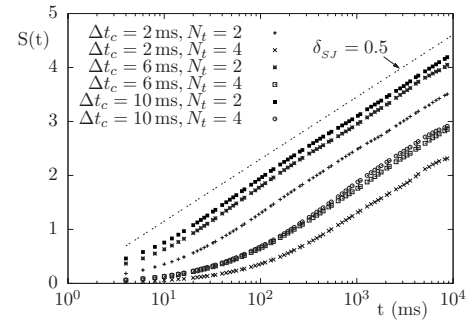


FIG. 1. $S(t)$ for rule no. 3 (SJ), for subject 6 with different choices of N_t and Δt_c .

ries) can be effectively selected out by noticing that the slope of the TS around a false RTP should be less steep than that around actual RTPs and should be similar to that of any other point in the TS. To filter out false RTPs we used the time derivative of the TS calculated by means of a convolution with a symmetrical window (50 msec wide) characteristic function (with value 1 inside the window, 0 outside). Looking at the modulus of the derivative signal, we remove segments (100 ms wide) centered around the time locations of the preliminary RTP and we estimate the probability density function of the remaining signal. On the basis of this distribution, a threshold aiming at discriminating actual from false RTP has been calculated as the 99th percentile of the distribution. Namely, we required that the TS at actual RTPs exhibits high slope absolute values that are uncommon among slopes of TS generic points. Needless to say that the application of this threshold criterion for the recognition of actual RTPs implies that only a portion of the occurring RTPs are detected.

C. Multichannel RTP detection

As mentioned above, the identification of RTPs that are concurrent among EEG channels (MC-RTPs) allows inferences about the dynamics of large-scale cortical interactions in recruitment/selection of neuronal populations forming metastable assemblies [43]. In fact, the *integrated* behavior of the brain is confirmed by the fact that RTPs simultaneously occur in two or more EEG channels more often than expected by chance [39]. The study of waiting times between MC-RTPs allows the estimation of the lifetime of the large-scale functional assemblies of neurons. For each EEG recording, the sequence of MC-RTPs is obtained from single-channel RTPs via the introduction of two thresholds: the first one, Δt_c , defines the maximum time distance for two single-channel RTPs (from different channels) to be considered concurrent; the second one, N_t , defines the minimum number of concurrent single-channel RTPs required for a MC-RTPs to be recorded as a global event. Since events that have a distance less than Δt_c are considered to be simultaneous, Δt_c must be small. We herein use, unless differently stated (e.g., in Figs. 1 and 5), Δt_c equal to the time resolution of our recording, namely, 2.0 ms. Analogously, unless differently stated, we take $N_t=2$.

IV. ANOMALOUS DIFFUSION

A. Diffusion entropy

Given a diffusion process

$$\dot{x} = \xi \Rightarrow \Delta x = \int_{t_w}^{t_w+\Delta t} \xi(t') dt', \quad (16)$$

the three rules determine the value of the variable ξ with respect to time t . For each rule we determine $p(\Delta x, \Delta t)$ and calculate the Shannon entropy of the diffusion process (hence the name diffusion entropy)

$$S(\Delta t) \equiv - \int_{-\infty}^{+\infty} p(\Delta x, \Delta t) \ln p(\Delta x, \Delta t) d\Delta x. \quad (17)$$

Using scaling condition (8), it is straightforward to prove that

$$S(\Delta t) = \delta \ln \Delta t + S_0, \quad (18)$$

where $S_0 = -\int_{-\infty}^{+\infty} F(x) \ln F(x) dx$. Notice that the scaling is in fact asymptotic, namely, it is only exact for $t \rightarrow \infty$. There is, however, always a time T denoting the time it takes for this asymptotic behavior to be reached. To take this property into account we assume

$$S(\Delta t) = \delta \ln(\Delta t + T) + S_0. \quad (19)$$

The DE method of analysis makes it possible for us to detect the scaling index δ by plotting the Shannon functional and thus determine δ by fitting the right-hand side of Eq. (19) to the data. Since the DE technique rests on a smooth evaluation of the distribution density, rule no. 2, corresponding to SV, is not numerically reliable due to data sparseness. In particular the support of $p(\Delta x, \Delta t)$ is as large as Δx assuming all possible values in the interval $[-\Delta t, \Delta t]$ with many ‘‘holes.’’ This is especially crucial for the DE analysis, which rests on the evaluation of the probability density function, and therefore, from a numerical standpoint, on the size of the histogram bins. On the other hand, for rules no. 1 (AJ) and no. 3 (SJ) DE rapidly converges, as the support of Δx keeps its compactness for larger values of Δt , with respect to rule no. 2 (SV). In these cases the results are stable for a wide range of bin sizes.

Let us now study how scaling detection changes with respect to different choices of the arbitrary thresholds N_t and Δt_c earlier defined in Sec. III. Let us recall that coincidences have been defined in Sec. III C as events characterized by at least two channels ($N_t=2$) exhibiting RTP within a time distance of $\Delta t_c=2.0$ ms, the sampling time of the EEG. Figure 1 shows that the detected scaling index δ is robust with respect to the choice of different threshold values for N_t and Δt_c . As an example, curves in Fig. 1 correspond to rule no. 3 and subject 6, and the detected value for δ is always $\delta \approx 0.5$. Remarkably, this robustness with respect to threshold values was confirmed also for rule no. 1 and for all subjects.

Figure 2 shows the DE in action for AJ and SJ for subjects 7 and 22. The two figures [Figs. 2(a) and 2(b)] are remarkably similar. We note that this condition of remarkable simi-

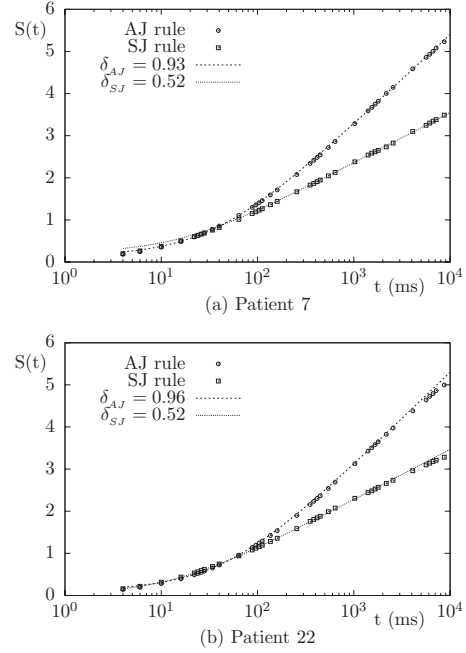


FIG. 2. Diffusion entropy $S(t)$ for rules no. 1 (AJ) and no. 3 (SJ) for subjects 7 and 22.

larity applies to all 30 subjects in our study; all of them yield the same fitting quality as that illustrated by Figs. 2(a) and 2(b).

As far as the scaling coefficients δ_{AJ} and δ_{SJ} are concerned, it is evident how close they are by examining the scatter plots shown in Fig. 3. Figure 3(a) shows that the detected values of δ_{AJ} , which in general can be any number in the interval $[0,1]$, are densely populated near the right limit of this interval, with values close to 1. Notice in fact that in Fig. 3(a) the δ_{AJ} axis was chosen between 0.75 and 1 to look for possible correlations between δ_{AJ} and δ_{SJ} in this limited range. Even more remarkably, δ_{SJ} , which in general

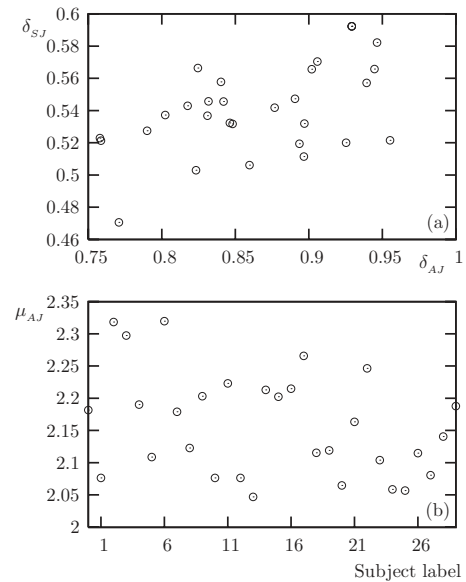


FIG. 3. (a) Scatter plot of δ_{AJ} vs δ_{SJ} . (b) Scatter plot of μ_{AJ} vs subject label.

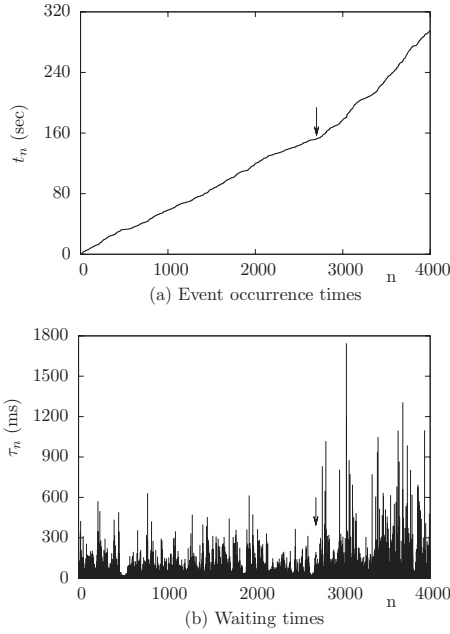


FIG. 4. (a) t_n vs n for subject 2. (b) τ_n vs n , same subject.

stands in the interval $[0,0.5]$, has, for almost all subjects, values slightly above 0.5. A $\delta_{SJ} > 0.5$ is a symptom of some statistical inaccuracy or of some drift, violating the assumption that the brain dynamics, although nonstationary, is driven by rules that do not change with time. We briefly discuss this point later in this section when describing Fig. 4. We are inclined to believe that these values indicate a $\delta_{SJ} \approx 0.5$, and therefore $\mu_{SJ} \geq 2$. The scatter plot of Fig. 3(a) does not show any correlation between the values of δ_{AJ} and δ_{SJ} , and therefore the different values detected in different subjects do not support indication of subject effect (namely different subjects having different μ), but rather a statistical spreading of the measured values, due to data limitation.

Although it is not possible to derive μ using rule no. 3 (SJ) alone, rule no. 1 (AJ), however, can be used to calculate a value of μ_{AJ} through the first equality of Eq. (11). This is shown in Fig. 3(b) as a function of the subject number.

In short, we evaluate the average μ_{AJ} over our set of subjects together with its standard deviation. We find $\bar{\mu}_{AJ} = 2.16$ with standard deviation 0.08. Therefore, we conclude that the DE analysis yields

$$\mu = 2.16 \pm 0.16 \quad (20)$$

at the 95% confidence level. Result (20) is based on Eq. (11), and therefore on the assumption that $\mu > 2$. This assumption is justified by the fact that $\mu < 2$ yields $\delta_{SJ} < 0.5$ in disagreement with our finding. However, from a theoretical viewpoint, it may be argued that some white or almost white noise is superimposed within the data yielding $\delta_{AJ} \approx 0.5$ even when $\mu < 2$. We therefore report the mean and standard deviation of μ_{AJ} calculated using Eq. (10) based on the assumption $\mu < 2$. These values are, respectively, $\bar{\mu}_{AJ} = 1.87$ with standard deviation 0.06 yielding $\mu = 1.87 \pm 0.12$. We see that in both cases the value of μ is close to 2.

As earlier mentioned, some discussion is in order about $\delta_{SJ} > 0.5$ shown in Fig. 3(a). Figure 4(a) shows t_n vs n for subject 2, where

$$t_n = \sum_{i=1}^n \tau_i \quad (21)$$

are the times at which events are detected, and τ_i is the time duration of the i th laminar region between two consecutive MC-RTP events (coincidences).

A straight line indicates a stationary rate of RTP. On the contrary, we see that there are two epochs with two different slopes graphically separated by a pointing-down arrow. Figure 4(b) confirms the same behavior by plotting τ_n vs n . This behavior is present in most subjects of our set. Subjects are in basal condition, namely, they are put at rest with closed eyes. In spite of the assumption that the process is renewal, and that the rules generating the times τ_n do not depend on time, it seems that the RTPs become less frequent after some time subjects are put at rest. From a signal-processing point of view, there is a nonstationarity, yet to be clarified, of a different kind of that generated by $\mu \approx 2$. A possible cause may be that putting a subject at rest with closed eyes corresponds to generating a slow switch from one to another condition thereby yielding the nonstationary drift depicted in Fig. 4. Regardless of its origin, this drift, however, explains why in most cases $\delta > 0.5$, even though this is a forbidden region for the SJ rule. In other words, the time evolution after the pointing-down arrow generates long laminar regions that produce uniform motion for very extended times, more extended than those generated by the renewal prescription with $\mu = 2$. We make the conjecture that these more extended laminar regions are the consequence of a systematic drift in EEG data and do not interfere with the renewal dynamics. For this reason in the next subsection we adopt the DFA method, which is well known for its capability of annihilating the consequences of systematic effects of this kind.

B. Detrended fluctuation analysis

In this subsection we briefly describe the DFA of Peng *et al.* [34]. The signal preprocessing is similar to that adopted for the DE, as both analyses rely on the diffusion processes stemming from the event identification with the help of the three rules for defining the “velocity” signal $\xi(t)$, or, better, $\xi(n)$, when n is a discrete time.

We then define a diffusion process X_n as

$$X_n = \sum_{i=1}^n [\xi(i) - \langle \xi \rangle], \quad (22)$$

where $\langle \xi \rangle$ is the global average of the signal, so that, being N total length of the signal, $X_0 = X_N = 0$. Next, X_t is divided into nonoverlapping time windows of length t , and, for each window, a local least-squares straight line fit (the local trend) is calculated by minimizing the squared error E^2 with respect to the slope and intercept parameters a and b , namely,

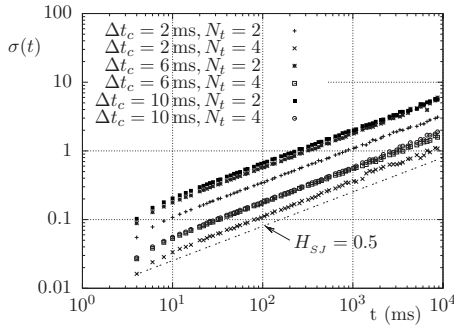


FIG. 5. $\sigma(t)$ for rule no. 3 (SJ), for subject 2 with different choices of N_T and Δt_c .

$$E^2 = \sum_{i=1}^t (X_i - ai - b)^2. \quad (23)$$

Next, the mean-square deviation from the trend, the fluctuation, is calculated over every window at every time scale:

$$F^2(t) = \frac{1}{t} \sum_{i=1}^t (X_i - ai - b)^2. \quad (24)$$

Finally, we average $F(t)$ over all windows and we notice that its root rescales as t^H , namely,

$$\sigma(t) = \sqrt{\frac{1}{N_{W \text{ windows}}} \sum F(t) \propto t^H}, \quad (25)$$

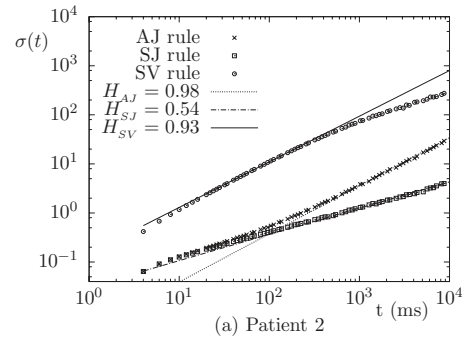
where $N_W = \lfloor N/t \rfloor$ is the number of the windows. This is expected, since, apart from the detrending procedure, this calculation is essentially a second-moment evaluation.

As done previously when illustrating the results of the DE analysis, we show the behavior for different threshold values. This is illustrated by Fig. 5 for subject 2 and for the SJ walker rule (rule no. 3). Also in this case we find $H_{SJ} \approx 0.5$, namely, $\mu \geq 2$.

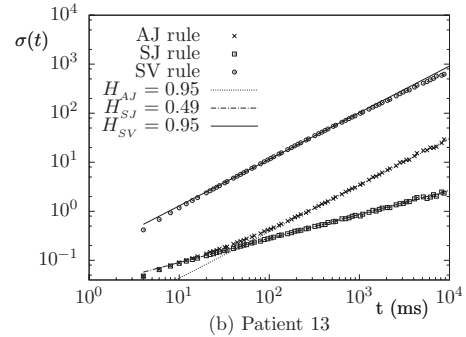
In Fig. 6 we show the DFA for four subjects with remarkably similar behaviors. Notice this is true for all of the 30 subjects, even the ones not shown. We have $H_{AJ} \approx 1$ and $H_{SJ} \approx 0.5$, establishing that $\mu \approx 2$, and therefore an ideal $1/f$ noise.

Notice that the DFA procedure does not require the calculation of the probability density function of the diffusion process, and therefore the procedure is not influenced by the compactness of the support of this density. It was, therefore, possible to use rule no. 2 or SV. It has to be noticed, however, that this rule becomes statistically unstable for large time windows with respect to the other rules. However, we see ballistic behavior for short and intermediate time windows, where we fitted H_{SV} to the data. As a result, we see that for all subjects in our set, we have that $H_{SV} \approx 1$. Figures 7 show this degree of universality via scatter plots of scalings H .

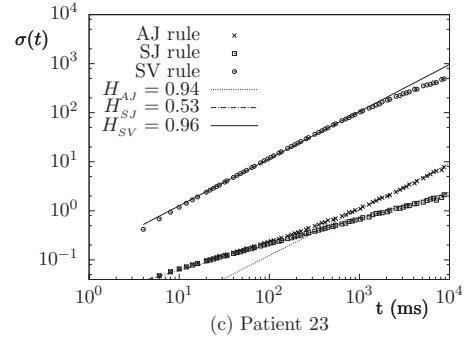
As expected, the results are not different from those stemming from DE. However, some further information can be extracted from this analysis. First of all, we see that DFA annihilates the observation-induced drift of Fig. 4, and the detected distribution of H_{SJ} is now centered around 0.5. This



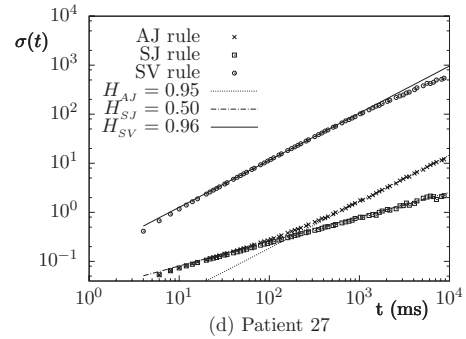
(a) Patient 2



(b) Patient 13



(c) Patient 23



(d) Patient 27

FIG. 6. DFA using the three rules for subjects 2, 13, 23, and 27. Sampling time (2 ms).

confirms that the behavior of Fig. 3 was induced by a non-stationary drift of the data, which was in fact able to affect the detected δ value but was not related to the renewal index μ of the underlying dynamics. No correlation is visible in any scatter plot of Fig. 7 proving that the spreading of the values is due to statistical limitation rather than subject effects. The fact that we may conclude that for each subject $H_{SJ} = 0.5$ leads us to the assumption $\mu \geq 2$. The results resemble the results earlier shown using DE, and our conjecture that $\mu \approx 2$ is therefore confirmed. We synthetically report the result for the AJ rule, as it is virtually able to span all

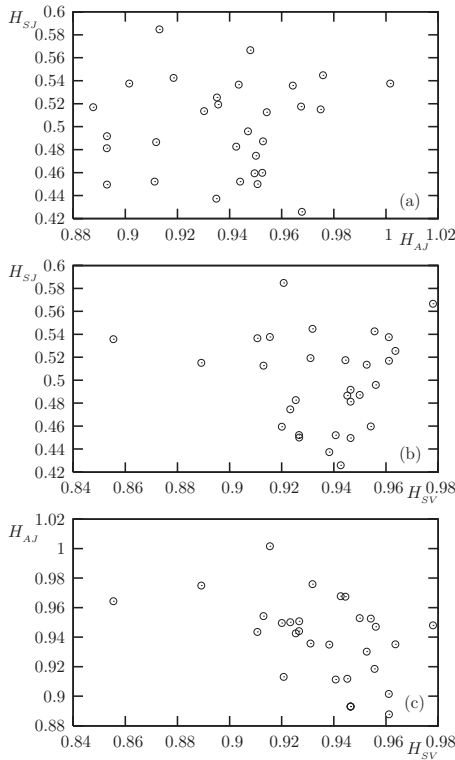


FIG. 7. Scatter plots: (a) H_{SJ} vs H_{AJ} ; (b) H_{SJ} vs H_{SV} ; (c) H_{AJ} vs H_{SV} .

the possible values in the interval (1,3). Also in this case we report the average and the standard deviation on our set of subjects. These are 2.12 and 0.06, respectively, yielding

$$\mu = 2.12 \pm 0.12 \quad (26)$$

at the 95% confidence level.

As earlier discussed in the case of the DE analysis, also in this case we have assumed $\mu \geq 2$, but we may also explore the case $\mu < 2$, imagining that a white noise superimposed to the data may yield $H_{SJ} \approx 0.5$ even in this case. The evaluation of the mean value of μ_{AJ} again yields $\bar{\mu}_{AJ} = 1.88$, with standard deviation 0.06, or, at the 95% confidence level, $\mu = 1.88 \pm 0.12$.

As earlier mentioned in Sec. II, the results stemming from the application of rule no. 1 (AJ) are ambiguous, even if in both cases μ is close to the boundary value $\mu = 2$. Let us now eliminate this ambiguity and calculate the index $\bar{\mu}$ stemming from walking rule no. 2 or SV. Equations (12) and (13) tell us that $\mu(H)$ is the same for both $\mu \geq 2$ and $\mu < 2$ [8]. We see that in all 30 cases we have that $\mu > 2$. The corresponding average index is $\bar{\mu}_{SV} = 2.13$, with standard deviation 0.05, so that

$$\mu = 2.13 \pm 0.10 \quad (27)$$

at the 95% confidence level, confirming both results (20) and (26) and proving that μ is slightly larger but close to 2.

It is worth pointing out that we limited ourselves to studying the closed-eye condition. The open-eye condition has been studied in an earlier work [8] using the DFA. It is of remarkable interest that these authors found H to be slightly

larger than 1. According to the theoretical analysis of Ref. [31] this is a consequence of the nonergodic nature of the condition $\mu < 2$ that makes H exceed the ballistic limit. Buiatti *et al.* [8] found that H changes from subject to subject with fluctuations from $H = 1.2$ to $H = 1.94$. The results of Fig. 6 show that our analysis of closed-eye subject by means of the DFA always yields $H < 1$ thereby confirming that the closed-eye condition corresponds to $\mu > 2$, although only slightly larger than 2. We also make the conjecture that, in addition to the nonergodic nature of $\mu \leq 2$, the transition from the open-eye to the resting state generated by the EEG analysis in the closed-eye condition may be a long-lasting process generating the observation-induced drift revealed by the results of Fig. 4.

Our conclusion is expressed by Eq. (26). We established the underlying existence of renewal crucial events by means of the fact that three independent analyses stemming from three different rules for constructing $\xi(t)$, studying either the scaling index δ or H , yield essentially identical results in Eqs. (20), (26), and (27). We further discuss this conclusion in Sec. VI.

V. RENEWAL AND MEMORY

The conclusion that the brain is characterized by renewal events, with $\mu \approx 2$, apparently conflicts with the observation that thinking requires highly correlated dynamics in both time and space. This observation seems to challenge the main result of this paper that the brain dynamics is driven by crucial events, namely, events with an inverse power-law distribution density and a power index μ that is contained in the middle of the interval of crucial events of Eq. (2). In fact, the renewal events, by definition, imply that the time intervals between two consecutive events are independent of each other thereby giving the misleading impression that the resulting process is incompatible with any form of memory. This observation is also the reason why the experimental discovery of $1/f$ noise in the brain [7,8] is not perceived as conflicting with the assumption of self-organization. In fact, on the one hand, the celebrated theory of self-organized criticality [44], which is frequently invoked for neurophysiological applications [36–38], was originally created to explain the origin of $1/f$ noise. On the other hand, the predominant view on the origin of $1/f$ noise is that it corresponds to fluctuating variables with extremely slow correlation functions [45]. Although the renewal approach to $1/f$ noise is not unknown in the literature [12], only recently it has become clear that the $1/f$ noise emerging from the transition to criticality is renewal [46]. The authors of Ref. [46] proved the $1/f$ noise emerging from the self-organization of defects in liquid crystals is incompatible with the existence of stationary correlation functions thereby implying the breakdown of ergodicity, a property frequently invoked in statistical physics.

First of all, let us explain why there is no contradiction between self-organization and renewal, and let us rather show that the brain dynamics, being determined by a process of self-organization, must produce renewal events. To support this claim we refer to the three recent papers [47–49].

The important paper [47] shows that the distribution of functional connections is generated by a scale-free network thereby suggesting a structural as well as a dynamical origin of the brain function, with the brain displaying an emergent state from a number of precise and successive events making the output of a brain highly reproducible and robust. However, the more recent paper [48] proves that these emergent properties are mainly dynamical rather than structural. In fact, Freiman *et al.* [48] show that the same scale-free properties as those observed by the authors of Ref. [47] are generated by the interactions of the nodes of a two-dimensional lattice, where each unit interacts with four nearest neighbors: a condition incompatible with the emergence of a topologically determined leadership. The scale-free network generated by the interacting spins of the Ising model of [48] is indistinguishable from the scale-free network emerging from the experimental observation in both [47,48].

The connections between the structural properties, whose dynamical origin is made compelling by the work of Ref. [48], and non-Poisson intermittence are established by the decision making model of Ref. [49]. This decision making model is similar to the Ising model of Ref. [48]. The single units are two-state systems, as in the case of Ref. [48], and the cooperation among the units is established by assuming that the nearest neighbors of a given unit generate a bias on the choice of each unit. In the case of all-to-all coupling with an infinite number of nodes this model generates the same ferromagnetic phase transition as the Ising model, although the cooperation strength is not expressed in terms of temperature. When the number of units is not infinite, the onset of phase transition is accompanied by non-Poisson fluctuations characterized by $\mu=1.5$, a value of the power index μ that in this case is predicted by an analytical treatment [49]. The renewal character of the intermittent process generated by the onset of phase transition has been carefully and accurately proved [49]. The connection between phase transition and non-Poisson and renewal intermittence is a general property of phase-transition process, as proved, for instance, by the authors of Ref. [50], who applied their theoretical approach directly to the Ising model.

On the basis of these remarks, we make the reasonable conjecture that the coincidences are a signature of the abrupt changes in structure configuration that must affect the patterns revealed by analysis [47,48]. In fact, all the nodes of Ref. [48] are equivalent. Moreover, it is not possible to justify the scale-free distribution of correlation-induced links without the assumption that this is a stable property corresponding to time-dependent structures. In such dynamic structures the leadership role, that is the role of hubs or stars, moves from one node to another in time without disrupting the regular topology used by the authors of Ref. [48]. The important work of Ref. [48] does not afford any direct information on the fluctuating dynamics of the network leaders, and we are convinced that the present paper suggests the proper theoretical perspective to fill this gap.

Finally, let us explain why the crucial renewal events rather than being incompatible with memory are, in a sense, a manifestation of memory much more extended than the widely quoted memory of relaxation processes without renewal events. Let us consider first the case $2 < \mu < 3$ and the

dichotomous fluctuation corresponding to rule no. 2 in the special case where all the sequences at $t=0$ are characterized by an event. This is a special preparation condition that serves the purpose of illustrating the surprising nature of these renewal processes. The autocorrelation function of the dichotomous fluctuation is given by [13]

$$\Psi(t_a = 0, t) = \left(\frac{T}{t+T} \right)^{\mu-1} \quad (28)$$

as a function of the argument t , which is set to 0 at the beginning of the observation process, whereas t_a is a parameter denoting the time interval between “preparation” (the first event) and “observation” ($t=0$). This analytical form is selected as the simplest form satisfying the normalization condition $\Psi(t_a=0, 0)=1$. When we make an experimental observation at very long times this correlation function becomes [13]

$$\Psi(t_a = \infty, t) = \left(\frac{T}{t+T} \right)^{\mu-2}, \quad (29)$$

and it is indistinguishable from the autocorrelation function of a fluctuation $\xi(t)$ with no crucial events

$$\Phi_{\xi}(t) = \left(\frac{T}{t+T} \right)^{\beta}, \quad (30)$$

which is frequently used [13] to explain the origin of the ideal $1/f$ noise for $\beta \rightarrow 0$, with the formula

$$\eta = 1 - \beta. \quad (31)$$

We see, however, that by identifying β with $\mu-2$, we recover the prescription of Eq. (4). This relationship between indices shows that crucial renewal events are compatible with the existence of memory as extended in time as the memory of the fluctuations with the slowest possible autocorrelation function.

Now, let us show that the crucial renewal events with $\mu < 2$ correspond to an even more extended memory. If we make the assumption that the aged autocorrelation function of Eq. (29) holds true also when $\mu < 2$ we obtain the apparently strange [51] condition of an autocorrelation function increasing rather than decreasing upon time increase. Although this is not a correct representation of the condition $\mu < 2$, it gives an intuitive understanding of the impressively extended time correlation of the renewal processes with $\mu < 2$. The correct approach to $1/f$ noise, in this case, rests on the evaluation of the waiting-time distribution density that, as shown in Ref. [16], has the following form:

$$\psi(t_a = 0, t) = (\mu - 1) \frac{T^{\mu-1}}{(t+T)^{\mu}} \quad (32)$$

as well as

$$\psi(t_a = \infty, t) \propto \frac{1}{(t+T)^{\mu-1}}. \quad (33)$$

In the case $\mu < 2$ the form of Eq. (33) is made compatible with the normalization requirement by the fact that the experimental sequence has a finite length L [16] thereby yield-

ing the unusual property of Eq. (6) with a noise intensity that becomes weaker with time and consequently with the increase in L .

VI. CONCLUDING REMARKS

The theoretical approach to $1/f$ noise emerging from the recent work of Refs. [15,16] rests on the assumption that only crucial events exist, namely, unpredictable quakes separated by time intervals, whose length is described by an inverse-power-law distribution density with index μ fitting the condition $1 < \mu < 3$. It is interesting to notice that the authors of Ref. [52] find for the time duration of phase-lock interval, or duration of coupling between a pair of neurophysiological processes, distribution densities with μ belonging to the same range. The condition of ideal $1/f$ noise emerges from the further idealized assumption that $\mu=2$. It is evident that the brain's complexity may largely depart from these idealizations mainly because a single-channel EEG is expected to depend only indirectly on crucial events. Moreover, setting the subjects in the basal state may generate a nonstationary drift in addition to the renewal nonstationarity associated with the condition $\mu \approx 2$.

The role of these disturbances has been significantly weakened by moving from the observation of single EEG processes to the statistical analysis of coincidences among the RTP of different channels (MC-RTP). The intuitive explanation of why coincidences are closer to crucial events is because crucial events are global properties of the brain as a whole [32], and the cognitive function of the brain is determined by the interaction among different areas [53]. However, focusing on coincidences is not yet enough to identify with absolute certainty the crucial events. The determination of occurrence time of a crucial event is affected by errors, which can be interpreted as the manifestation of a perturbing noise. This explains why in the short-time region the scaling H determined by using the DFA method is very close to the ordinary value $H=0.5$ regardless of whether we use rule no. 1 (AJ), which, with no noise disturbance, should generate anomalous scaling ($H \neq 0.5$), or rule no. 3 (SJ), which, on the contrary, in the same ideal condition should yield ordinary scaling in the whole region $\mu > 2$. It is easy to prove that the addition of noisy perturbation to the crucial events generates a diffusion process that in the long-time limit is dominated by anomalous scaling. Extensive analyses not reported here [40], both on single-channel RTPs and on MC-RTPs, confirm that the renewal character of the signal can be measured using the procedure of Ref. [54]: the resulting renewal index (defined in [55]) is not consistent with perfect renewal, but only with *partial renewal*. In other words, noise breaks down the renewal character of detected events, therefore, preventing a direct evaluation of μ from $\psi(t)$, but, as established in [56], does not change the diffusion scaling indexes H and δ of the underlying renewal process.

In addition to the errors affecting the crucial event detection, we have to take into account the statistical fluctuations generated by the lack of a sufficiently large number of crucial events. This has the effect of making the statistics behind rule no. 2 (SV) too poor for the diffusion process to correctly

generate $H=1$. In fact, in the long-time limit the probability distribution density generated by rule no. 2 is very broad thereby generating statistical inaccuracy, whereas with the adoption of the AJ model, rule no. 1, the broadening is made more moderate by the systematic shift of the distribution density [28]. The adoption of the DFA method has the benefit of annihilating the observation-induced nonstationary effects that make the scaling δ detected by the DE method fluctuate around a value significantly larger than 0.5. However, at the same time the DFA method may generate the misleading impression that the long-time scale yields a regression to ordinary statistics, if only rule no. 2 was adopted. In spite of the misleading information generated by the action of events that are not the genuinely crucial events, hypothesized by the $1/f$ -law theory [15,16], we did succeed in determining the power index μ of the brain's dynamics as a result of a trade-off among DE, DFA, and three walking rules.

In conclusion, we have established that the brain's dynamics at rest is characterized by crucial events with $\mu=2$, or slightly larger, with an error of about 7%. We hope that the assessment of this property may have interesting interdisciplinary consequences. First of all we note that $\mu=2$, or slightly larger, is the same fractal index as that involved in language [25,27] thereby suggesting that the brain's dynamics is the ultimate origin of Zipf's law. At this level it is extremely interesting to notice, for instance, that the study of language in schizophrenics is associated with an anomalous Zipf's law [57], and hence with an alteration of its renewal index μ [25]. From an inferential point of view this is in line with the hypothesis of Feinberg and Guazzelli [58] on alteration of functional connectivity in cortical and subcortical structures. Making the conjecture that it is possible to identify the μ of the language and the μ of EEG dynamics in schizophrenic patients may lead to the design of methods for the therapists to establish efficient interactions with these patients, and, hopefully, new therapeutic strategies.

It is important to stress that in the literature the emergence of $1/f$ noise from the brain dynamics is widely recognized. In addition to the earlier quoted papers, we would like to mention also the work of Refs. [59,60]. These papers establish a correspondence between the emergence of $1/f$ noise and phase-transition processes [61] thought to be a natural outcome of self-organized criticality [60]. The correlation between neural activity and the emergence of slow fluctuations [62] affords another clue for the origin of $1/f$ noise and for the origin of memory discussed in Sec. V. Does this paper conflict with this literature? Although this literature, as earlier pointed out, ignores the role of renewal events, this does not necessarily imply that there is a conflict between the perspective outlined in this paper and this literature. As a relevant example, we would like to quote Ref. [63]. The authors of this interesting paper show that slowly driven systems can evolve to a self-organized critical state yielding $1/f^\eta$ noise. They claim that the dynamics discussed in their paper cannot be reduced to a renewal process with a power-law distribution of waiting time. This would imply a conflict with the perspective adopted in this paper. Yet, the work of Ref. [63] is closely related to an earlier work [64], where interevent time distances with an inverse power law appear. These events are characterized, in the case of samples of size

large enough, by vanishing Lyapunov coefficients, a sign of their renewal nature [65]. On the one hand, affording a compelling proof of the existence of leading events of renewal nature is a hard task [54] given the fact that they may be embedded in a cascade of nonrenewal events that obscure the real nature of the crucial events, even though they are the cause of this cascade [66]. On the other hand, it is worthwhile to discuss the possible consequences of the renewal nature of the brain.

The determination of the renewal nature of the brain's dynamics should make it possible to go beyond the generic observation that the brain is a source of $1/f$ noise and is most sensitive to $1/f$ stimuli. In fact, the CM principle [13] is an attractive conjecture that has been recently proved by means of rigorous theoretical arguments [67]. It is now well understood that the information transfer from one complex network to another becomes maximally efficient if both systems are driven by crucial events with $\mu=2$. The CM effect can be used to explain the influence of arts on the brain. In fact, according to Yevin [68] both artistic compositions and the brain are systems in the critical condition thereby realizing the condition for the optimal information transport behind the CM effect [67].

As far as the contribution to the brain's neurophysiology is concerned, we have found a stable $1/f$ spectrum dominating brain dynamics of healthy awake subjects during a minimal-stimulation condition. This is a special condition since relaxed individuals were asked to avoid structured thoughts, so that memories and thoughts would freely emerge, without any influence of external stimuli. In our future investigations we shall verify if the scale-free characteristic of brain dynamics is a brain structural property or a behavior-dependent property. As extreme condition of environment disconnection, the $1/f$ rule could be verified during sleep. Also the study of brain dynamics during stimulations could be useful, since it may lead us to establish that the brain's sensitivity to $1/f$ noise is a manifestation of the CM principle [67] which makes $1/f$ systems maximally sensitive to $1/f$ stimuli. Thus, the recognition that the brain's dynamics is a generator of ideal $1/f$ noise is expected to open the door to the design of the proper stimuli for therapeutic purposes.

ACKNOWLEDGMENT

P.G. thankfully acknowledges financial support from USARO through Grant No. W911NF-08-1-0177.

-
- [1] H. Kadota, K. Kudo, and T. Ohtsuki, *Neurosci. Lett.* **370**, 97 (2004).
- [2] L. M. Ward, *Dynamical Cognitive Science* (MIT Press, Cambridge, MA, 2002), p. 152.
- [3] D. L. Gildea, T. Thornton, and M. W. Mallon, *Science* **267**, 1837 (1995).
- [4] J. M. Medina, *Phys. Rev. E* **79**, 011902 (2009).
- [5] S. Bianco, E. Geneston, P. Grigolini, and M. Ignaccolo, *Physica A* **387**, 1387 (2008).
- [6] G. Werner, *Biosystems* **96**, 114 (2009).
- [7] K. Linkenkaer-Hansen, V. V. Nikouline, J. M. Palva, and R. J. Ilmoniemi, *J. Neuroscience* **21**, 1370 (2001).
- [8] M. Buiatti, D. Papo, P.-M. Baudonnière, and C. van Vreeswijk, *Neuroscience* **146**, 1400 (2007).
- [9] C. T. Kello, B. C. Beltz, J. G. Holden, and G. C. Van Orden, *J. Exp. Psychol. Gen.* **136**, 551 (2007).
- [10] L. Lemoine, K. Torre, and D. Delignières, *Can. J. Exp. Psychol.* **60**, 247 (2006).
- [11] D. R. Cox, *Renewal Theory* (Methuen & Co. Ltd., London, 1962).
- [12] S. B. Lowen and M. C. Teich, *Phys. Rev. E* **47**, 992 (1993).
- [13] B. J. West, E. L. Geneston, and P. Grigolini, *Phys. Rep.* **468**, 1 (2008).
- [14] Actually, the authors of Ref. [12] adopt an alternate sequence of two distinct values equivalent to the alternate sequence of 1 and -1 . Thus, the laminar regions created by the procedure adopted in this paper are more extended than the original ones. It is well known that the new sequence of laminar regions has the same inverse power-law behavior as the original sequence.
- [15] G. Margolin and E. Barkai, *J. Stat. Phys.* **122**, 137 (2006).
- [16] M. Lukovic and P. Grigolini, *J. Chem. Phys.* **129**, 184102 (2008).
- [17] Y. Yu, R. Romero, and T. S. Lee, *Phys. Rev. Lett.* **94**, 108103 (2005); R. Soma, D. Nozaki, S. Kwak, and Y. Yamamoto, *ibid.* **91**, 078101 (2003).
- [18] J. Alvarez-Ramirez, C. Ibarra-Valdez, E. Rodriguez, and L. Dagdug, *Physica A* **387**, 281 (2007).
- [19] S. Bianco, M. Ignaccolo, M. S. Rider, M. J. Ross, P. Winsor, and P. Grigolini, *Phys. Rev. E* **75**, 061911 (2007).
- [20] H. D. Jennings, P. Ch. Ivanov, A. de M. Martins, P. C. da Silva, and G. M. Viswanathan, *Physica A* **336**, 585 (2004).
- [21] F. H. Rauscher, G. L. Shaw, and K. N. Ky, *Nature (London)* **365**, 611 (1993).
- [22] J. I. Gold and M. N. Shadlen, *Annu. Rev. Neurosci.* **35**, 535 (2007).
- [23] C. F. Camerer, *Neuron* **60**, 416 (2008).
- [24] P. A. Samuelson, *The Foundations of Economics Analysis* (Harvard University Press, Harvard, Cambridge, MA, 1947).
- [25] P. Allegrini, P. Grigolini, and L. Palatella, *Chaos, Solitons Fractals* **20**, 95 (2004).
- [26] M. E. Bales and S. B. Johnson, *J. Biomed. Inf.* **39**, 451 (2006).
- [27] R. F. Cancho and R. V. Solé, *Proc. Natl. Acad. Sci. U.S.A.* **100**, 788 (2003).
- [28] P. Grigolini, L. Palatella, and G. Raffaelli, *Fractals* **9**, 439 (2001).
- [29] P. Grigolini, D. Leddon, and N. Scafetta, *Phys. Rev. E* **65**, 046203 (2002).
- [30] R. Metzler and J. Klafter, *Phys. Rep.* **339**, 1 (2000).
- [31] A. K. Kalashyan, M. Buiatti, and P. Grigolini, *Chaos, Solitons Fractals* **39**, 895 (2009).
- [32] W. Singer, *Eur. Rev.* **17**, 321 (2009).
- [33] N. Scafetta and B. J. West, *Phys. Rev. Lett.* **92**, 138501 (2004).

- (2004).
- [34] C.-K. Peng, S. V. Buldyrev, S. Havlin, M. Simons, H. E. Stanley, and A. L. Goldberger, *Phys. Rev. E* **49**, 1685 (1994).
- [35] M. Martin, *Scientist* **22**, 23 (2008).
- [36] D. Plenz and T. C. Thiagarjan, *Trends Neurosci.* **30**, 101 (2007).
- [37] J. M. Beggs and D. Plenz, *J. Neurosci.* **23**, 11167 (2003).
- [38] D. R. Chialvo, *New Ideas Psychol.* **26**, 158 (2008).
- [39] A. Ya. Kaplan, A. A. Fingelkurts, A. A. Fingelkurts, S. V. Borisov, and B. S. Darkhovsky, *Signal Process.* **85**, 2190 (2005).
- [40] D. Menicucci *et al.* (unpublished).
- [41] N. E. Huang *et al.*, *Proc. R. Soc. London, Ser. A* **454**, 903 (1998).
- [42] B. E. Brodsky, B. S. Darkhovsky, A. Ya. Kaplan, and S. L. Shishkin, *Comput. Methods Programs Biomed.* **60**, 93 (1999).
- [43] A. A. Fingelkurts and A. A. Fingelkurts, *Cogn. Process.* **7**, 135 (2006).
- [44] P. Bak, C. Tang, and K. Wiesenfeld, *Phys. Rev. Lett.* **59**, 381 (1987).
- [45] R. Voss and J. Clarke, *Phys. Rev. Lett.* **36**, 42 (1976).
- [46] L. Silvestri, L. Fronzoni, P. Grigolini, and P. Allegrini, *Phys. Rev. Lett.* **102**, 014502 (2009).
- [47] V. M. Eguíluz, D. R. Chialvo, G. A. Cecchi, M. Baliki, and A. V. Apkarian, *Phys. Rev. Lett.* **94**, 018102 (2005).
- [48] D. Fraiman, P. Balenzuela, J. Foss, and D. R. Chialvo, *Phys. Rev. E* **79**, 061922 (2009).
- [49] M. Turalska, M. Lukovic, B. J. West, and P. Grigolini, *Phys. Rev. E* **80**, 021110 (2009).
- [50] Y. F. Contoyiannis and F. K. Diakonou, *Phys. Lett. A* **268**, 286 (2000).
- [51] We say apparently strange because the velocity autocorrelation function in turbulent fluid flow does increase in this way.
- [52] M. G. Kizbichler, M. L. Smith, S. R. Christensen, and E. Bullmore, *PLOS Comput. Biol.* **5**, 1 (2009).
- [53] G. Tononi, *BMC Neurosci.* **5**, 42 (2004).
- [54] P. Allegrini, F. Barbi, P. Grigolini, and P. Paradisi, *Phys. Rev. E* **73**, 046136 (2006); *Chaos, Solitons Fractals* **34**, 11 (2007); P. Paradisi, R. Cesari, and P. Grigolini, *Cent. Eur. J. Phys.* **7**, 421 (2009).
- [55] S. Bianco, P. Grigolini, and P. Paradisi, *J. Chem. Phys.* **123**, 174704 (2005).
- [56] P. Allegrini, M. Barbi, P. Grigolini, and B. J. West, *Phys. Rev. E* **52**, 5281 (1995); P. Allegrini, P. Grigolini, and B. J. West, *Phys. Lett. A* **211**, 217 (1996); N. Scafetta, V. Latora, and P. Grigolini, *Phys. Rev. E* **66**, 031906 (2002).
- [57] W. Piotrowska and X. Piotrowska, *J. Quant. Linguist.* **11**, 133 (2004).
- [58] I. Feinberg and M. Guazzelli, *Br. J. Psychiatry* **174**, 196 (1999).
- [59] W. J. Freeman, *Clin. Neurophysiol.* **117**, 572 (2006).
- [60] W. J. Freeman, *Biol. Cybern.* **92**, 350 (2005).
- [61] R. Kozma and W. J. Freeman, *Neurocomputing* **44-46**, 1107 (2002).
- [62] A. Shmuel and D. A. Leopold, *Hum. Brain Mapp.* **29**, 751 (2008).
- [63] J. Davidsen and M. Paczuski, *Phys. Rev. E* **66**, 050101(R) (2002).
- [64] M. de Sousa Vieira, *Phys. Rev. E* **61**, R6056 (2000).
- [65] P. Allegrini, V. Benci, P. Grigolini, P. Hamilton, M. Ignaccolo, G. Menconi, L. Palatella, G. Raffaelli, N. Scafetta, M. Virgilio, and J. Yang, *Chaos, Solitons Fractals* **15**, 517 (2003).
- [66] M. S. Mega, P. Allegrini, P. Grigolini, V. Latora, L. Palatella, A. Rapisarda, and S. Vinciguerra, *Phys. Rev. Lett.* **90**, 188501 (2003).
- [67] G. Aquino, M. Bologna, P. Grigolini, and B. J. West (unpublished).
- [68] I. Yevin, *Complexus* **3**, 74 (2006).